

Monte Carlo simulation on the influence of aberration on the propagation characteristics and coupling efficiencies for a single-mode fiber to a slab waveguide coupling system

SHUPING LI^{a,b}, JINGPING ZHU^{a*}, YUZHOU SUN^a, TIAN TONG TANG^a, WANGUANG QIN^a

^aKey Laboratory for Physical Electronics and Devices of the Ministry of Education and Shaanxi Key Lab of Information Photonic Technique, Xi'an Jiaotong University, Xi'an 710049, China

^bSchool of Information Engineering, Tibet Institute for Nationalities, Xianyang, Shaanxi, 712082, China

For the butt-joint coupling between a single mode fiber (SMF) and a single mode dielectric slab waveguide (SMDSW) with a spherical fiber micro-lens (SFML), the influence of the aberration on the propagation characteristics and coupling efficiencies of the coupler are investigated by Monte Carlo simulation. Simulation results show that because of spherical aberration effects, the location of the waist of the focused beam is nearer to the geometrical focus than that of the aberration free fiber micro-lens (AFFML). And the coupling efficiencies less and the curves platter with respect to the AFFML.

(Received May 23, 2011; accepted June 9, 2011)

Keywords: Waveguide, Fiber, Microlens, Coupling system

1. Introduction

With the development of integrated optical technology, a variety of integrated waveguide devices are applied in communication systems. When a single mode fiber is directly butt-coupled to a photonic device, there is a 7–10 dB power loss and submicron alignment tolerances are required. To achieve the low coupling loss, it is necessary to transform the mode on chip to better match that of the fiber. Using this concept, various integrated mode transformer solutions have been proposed. However, most of these approaches still involve complex growth and processing steps. Micro-lenses which are fabricated directly on the end faces of single-mode fibers (SMFs) have been used because they can produce high coupling efficiencies between the single mode optical fiber (SMF) and the single mode dielectric slab waveguides (SMDSW) in guided wave circuits [1-6]. Because spherical fiber micro-lens (SFML) fabrication is simpler and faster than other fiber micro-lenses, the SFML is often used in coupling system.

In the past decades, the butt-coupling characteristics of fibers with waveguides have been theoretically investigated by numerical methods such as finite difference time domain (FDTD) [7] and the overlap integral method [8]. Based on the overlap integral method and using the Gaussian and modified Gaussian approximation of single mode fibers and waveguides, simple analytical formulas have been presented. However, this simple method can not take the reflection loss, the diffraction loss is not considered yet, and the influence of the spherical aberration on the efficiency can not

calculated. Rigorous numerical methods require generally large computation resources, and a 3D simulation is time consuming. Because the SMF and the SMDSW have different symmetries, for a coupler of a SMF to a SMDSW coupling with a SFML, it is difficult to calculate the electromagnetic field distribution and coupling efficiency using a simple analytic method. Monte Carlo methods are widely used in simulating physical and mathematical system, and the methods can be used to solve many problems that traditional deterministic methods cannot.

In this paper, the propagation and coupling characteristics of a SMF and a LiNbO₃ or silicon-based SMDSW coupling with a SFML is simulated using the Monte Carlo simulation method. The influence of the spherical aberration on the spot sizes and the radial intensity distribution of the focused beam will be analyzed, and the influence of the aberration on the coupling efficiencies is also discussed.

2. Theories

In a cylindrical coordinate, for a single mode fiber, the mode power of radial distribution and angular distribution are [9]

$$f(r) = \begin{cases} r \frac{\beta}{2\omega\mu} |A|^2 J_0^2(hr) & r \leq a \\ r \frac{\beta}{2\omega\mu} |B|^2 K_0^2(qr) & r > a \end{cases} \quad (1)$$

$$f(\vartheta) = \frac{1}{2\pi} \tag{2}$$

where

$$h = \sqrt{n_1^2 k_0^2 - \beta^2}, \quad q = \sqrt{\beta^2 - n_2^2 k_0^2}, \quad B = \frac{AJ_0(ha)}{K_0(qa)},$$

$$k_0 = \frac{\omega}{c} \tag{3}$$

The beam along the single mode fiber propagates through the SFML, according to the phase transformation formula, the diffraction field can be written as

$$U'(x_1, y_1) = f(x_1, y_1) \exp\left[-\frac{jk}{2f}(x_1^2 + y_1^2)\right] P(x_1, y_1) \tag{4}$$

$P(x_1, y_1)$ is the formula for function of the pupil. The expression $f(x_1, y_1)$ describes the radial distribution function in the rectangular coordinate system. And the intensity distribution is

$$I(x, y) = \left| \frac{\exp(jkz)}{j\lambda z} \iint_{-\infty}^{\infty} U'(x_1, y_1) \exp\left[jk \frac{(x-x_1)^2 + (y-y_1)^2}{2z}\right] dx_1 dy_1 \right|^2 \tag{5}$$

3. Monte Carlo modeling

The coupler of a SMF to a SMDSW coupling with a SFML is shown in Fig.1. The incident light propagates

through a SFML, and can be considered as a signal passing through the two irrelevant systems. One system includes the aberration effect, and another includes the diffraction effect. The image can be described as a convolution of the object upon response of the two systems, and modeling is performed according to the following steps:

A . The incident light obeys the probability distribution functions (1) and (2), we generated a random number from the probability distribution function by method of acceptance-rejection. Then , the initial coordinates (x_0, y_0) of the incident ray are defined.

B . The direction of propagation and the coordinates (x_1, y_1) of the exit ray can be calculated via a ray trajectory formula. And there is perturbation generated by the diffraction of the lens aperture, the perturbation are a random variable with probability distribution (5). The trajectories of the exit ray are treated as the sum of the geometrical trajectories plus perturbation terms caused by the diffraction effects. Therefore, the coordinates (x_2, y_2) of the ray in the observed plane (the end-face of the SMDSW) can be written as

$$x_2 = x_1 + \delta x \tag{6}$$

$$y_2 = y_1 + \delta y \tag{7}$$

where δx and δy are the perturbation terms, respectively.

C . These refraction rays launch into the SMDSW, and only certain light that satisfies the wave guiding conditions that can propagate in the waveguide.

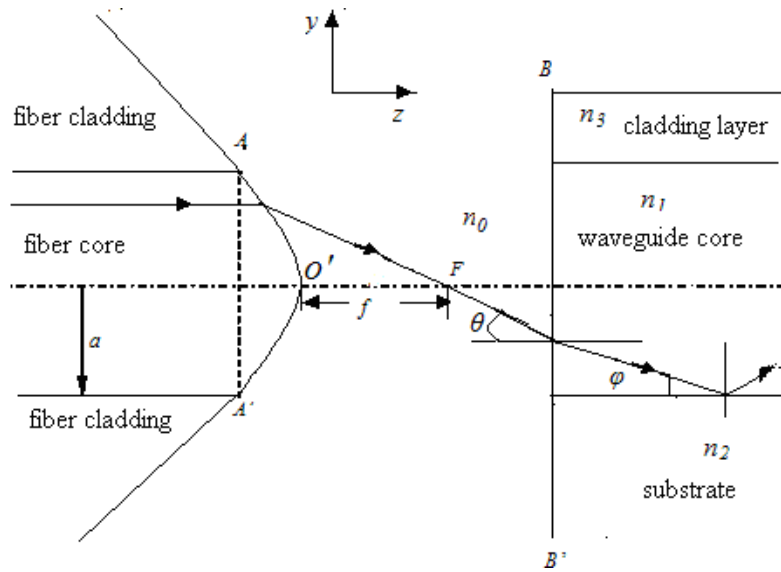


Fig.1. Propagation of an optical ray through the coupling systems.

4. Program test

The random sample number of incident rays is 80,000. The sample rays propagate through the fiber end-face micro-lens' and produce a spot in the observe plane. The spot size W_s is defined as is the radius within which 84% of the photon energy is enclosed. In order to estimate the spot size and the waist position accurately, five trials are used in each case and the average results of the five trials.

The program consists of two main programs, and the program for random sampling of the incident photons is tested first. The statistical radial intensity distributions are shown in Fig.2, and the results calculated by (1) are also given. It is clear that the simulation results are in excellent agreement with the calculated one.

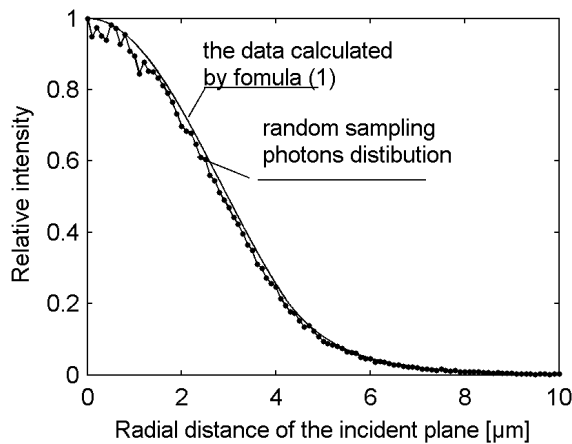


Fig. 2. Radial relative intensity of the incident beam in the incident plane.

The second step tests the ray tracing program. For a classic example of a spherical aberration calculation, we assumed a uniform plane wave with wavelength $1.55 \mu m$ incidents on a plano-convex lens with refractive index $n=1.46$, and radius of curvature $R=10 \mu m$. The distance of the random sampling ray from the optical axis was about $4 \mu m$, and the location on the axis was at $z=27.7378 \mu m$, as we can see from Fig.3. These simulation results are also in excellent agreement with the calculated data.

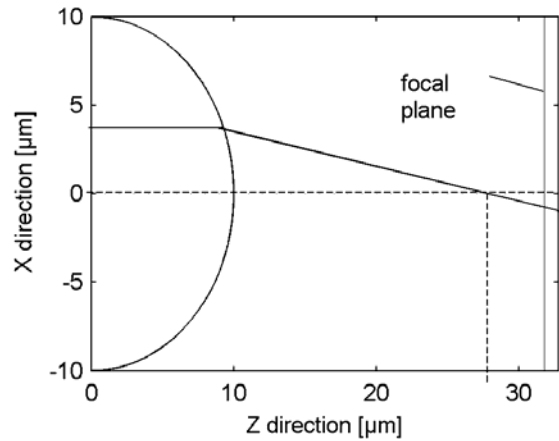


Fig.3. Simulation result of the axis spherical aberration.

From the above results, it is clearly shown that the program is both numerically stable and accurately calculated. The optical propagation characteristics of the fiber end-face micro-lens are simulated using these programs, and simulation results are shown

5. Simulating of the SFMLs

The spot size is a function of the propagation distance for the AFFML and the SFML as shown in Fig.4. For the SFML, the waist width is smaller, and the location of the waist is closer to the focus.

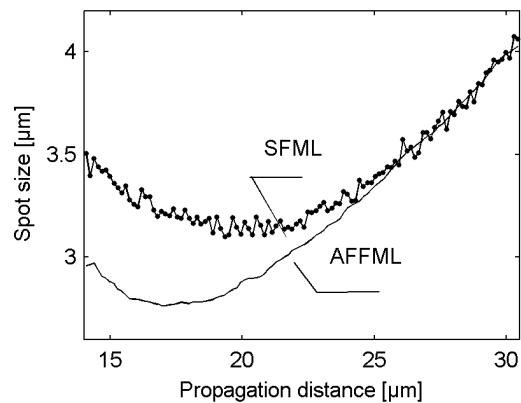


Fig.4. Spot size as a function of the propagation distance for the FML with curvature radius $R = 14 \mu m$.

For more knowledge about the effects of increasing the focal length on the spot size, the spot sizes of the focused beam for AFFML and SFML are shown in Fig.5. The spot size of the geometrical focal plane is larger than that of the waist plane for the SFM. And the spot size of the waist for the SFM is also larger than that for the AFFM, and the larger the spherical aberration, the larger the focused beam waist radius.

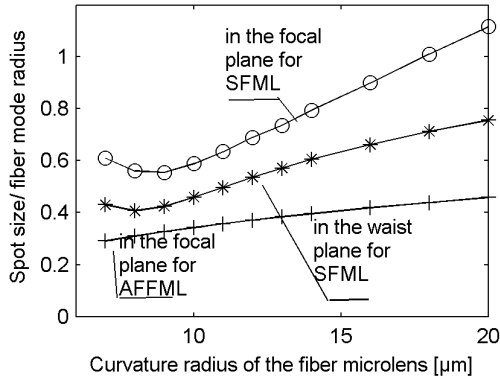


Fig. 5. Spot size of the focused beam for the AFFML and the SFML.

In general, for the AFFML, location of the waist of the focused beam is at the point of axial maximum intensity, however, for the SFML, in Fig.6, it is very clearly that the position of the axial maximum intensity does not coincide with the waist position, and shifts towards the position of the waist if R is lesser. Because of spherical aberration effects, the position of the axial maximum intensity does not coincide with the waist position and the geometrical focus.

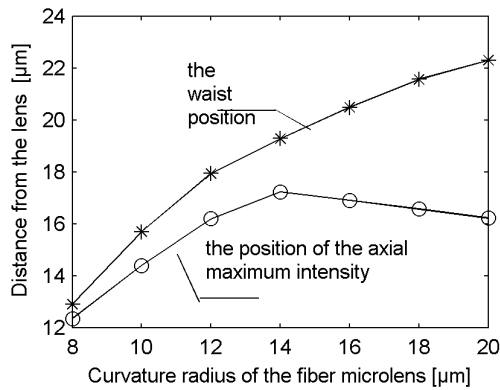


Fig.6. Comparing the positions of the waist and the maximum intensity along the axis.

From above discussion, we know that the spherical aberration affects on the the waist position of the focused beam, and it is called focal shift that the shift of the waist position deviates from the geometrical focus. For a AFFML, it is well known that the focal shift is a function of the Fresnel number associated with the diffracting aperture radius. For a comparison, the focal shift covers for the AFFML and the SFML are shown in Fig.7, respectively. For the AFFML, the relative focal shift is calculated by the formula (6) in [10], and the coefficients $m_1=0.3$ and $m_2=0.08$ are advised by the author.

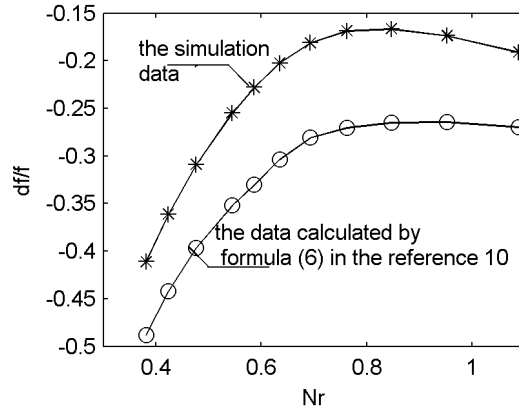


Fig.7. The focal shift as a function of the Fresnel number associated with the diffracting aperture radius.

The location of the waist is more closed to the geometrical focus for the SFML, and the relative focal shift of the SFML is less than that of the AFFML. The influence of the spherical aberration on the focused beam is further confirmed in Fig.7.

To show the effects of spherical aberration on the radial intensity distributions of the focused beams, numerical calculations for various curvature radii lens are carried out. Fig.8 illustrates the intensity distributions for SFMLs with different curvature radii. Because of the spherical aberration effect, the peak intensities are not located in the optical axis, and the intensity curves have two maxima. The curves of the intensity distribution in both the plane of the waist and the axial maximum intensity are not completely same. With the curvature radius increasing, the spherical aberration effect decreases, and diffraction effect grows, altering the point of axial maximum intensity gradually towards that of waist, and the intensity distribution curves are nearly identical. Therefore, the spot sizes in both the axial maximum intensity and waist planes are almost equal.

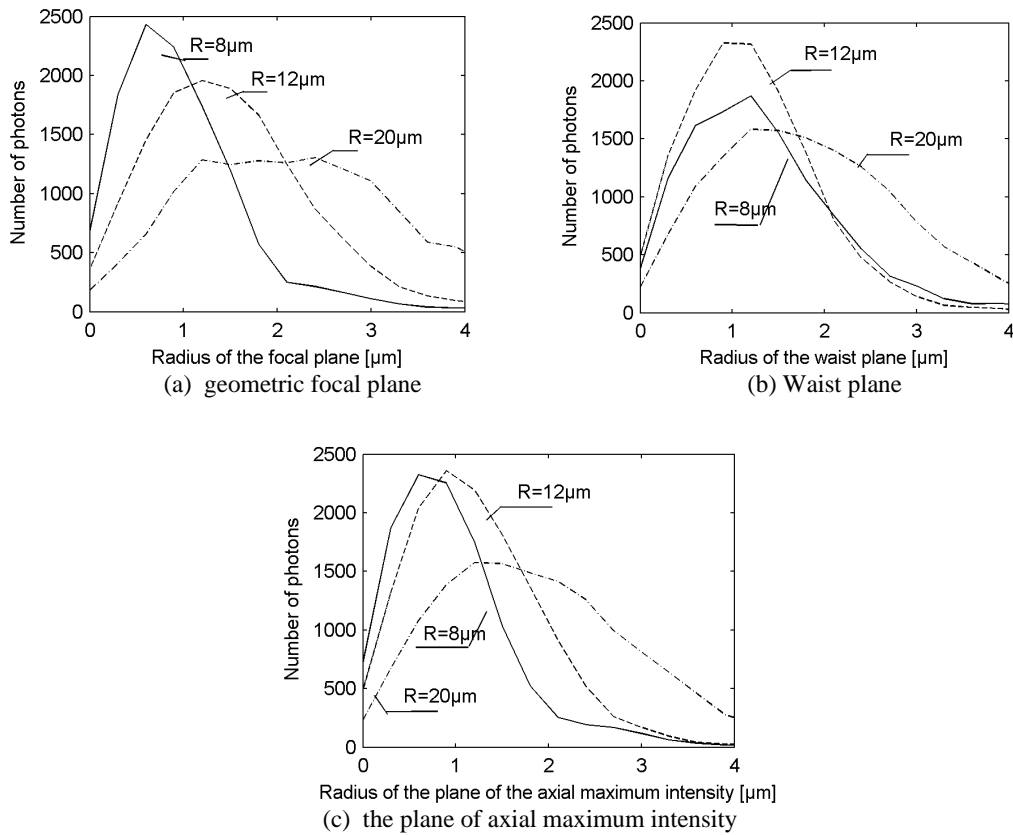


Fig. 8. Radial intensity distribution in the observe plane.

6. Coupling efficiencies

From above discussion, it is known that the intensity distribution curve of the SFML is absolutely different from mode distribution of the SMF. Because of this significant difference, it is not valid to calculate the coupling efficiency using an overlap integral method. In the coupler, the ratio of the number of the rays is satisfied by the wave guiding conditions and the number of incident rays is defined as coupling efficiency.

In the following section, the coupling characteristics of a SMF and a LiNbO₃ or silicon-based SMDSW coupling with a SFML are simulated. And in the numerical model, the refractive index of core and substrate LiNbO₃ SMDSW are 2.148 and 2.138 respectively, and that of SiO₂/Si SMDSW are 1.454 and 1.445 respectively. The material for the cladding layers of the two slab waveguides is air.

The coupling efficiency of a specific SMF coupling to the LiNbO₃ SMDSW is shown in Fig.9. When the core thickness of the SMDSW is 5 μm and the end-face of the waveguide is in the geometrical focal plane and the coupling efficiencies are in the region of 48%~67%, the maximum coupling efficiency located at r=10 μm, the corresponding focal length is about 21.49 μm. If the end-face is in the waist plane, the coupling efficiencies are in the region of 65%~77%, the maximum coupling efficiency

located at r=12 μm, the corresponding focal length is about 25.79 μm.

It is very clearly that when the end-face of the SMDSW lies in the waist plane, the coupling efficiencies are higher compared to the end-face lying in the geometric focal plane. The coupling efficiency curves are also shown to be flatter than that of end-face waveguides in a geometric plane. And the points of the maximum coupling efficiency don't match together.

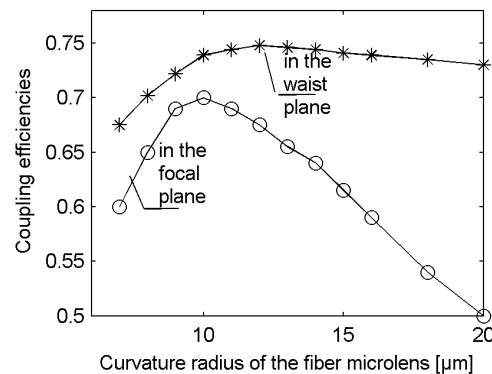


Fig. 9. Coupling efficiencies for coupling the SMF to LiNbO₃ SMDSW with SFML.

The coupling efficiency curves of the SMF and the LiNbO₃ and the silicon-based SMDSW coupling with the SFMLs respectively are given in Fig.10. For the coupler of the SMF to the SiO₂/Si SMDSW coupling with the SFML, when the waveguide core thickness is 5 μ m, the coupling efficiencies are in the region of 53.5%~63.8%, it is can be seen that the coupling efficiency is less than that of LiNbO₃ SMDSW. And the maximum coupling efficiency located at $r=15\mu$ m, the corresponding focal length is about 32.24 μ m.

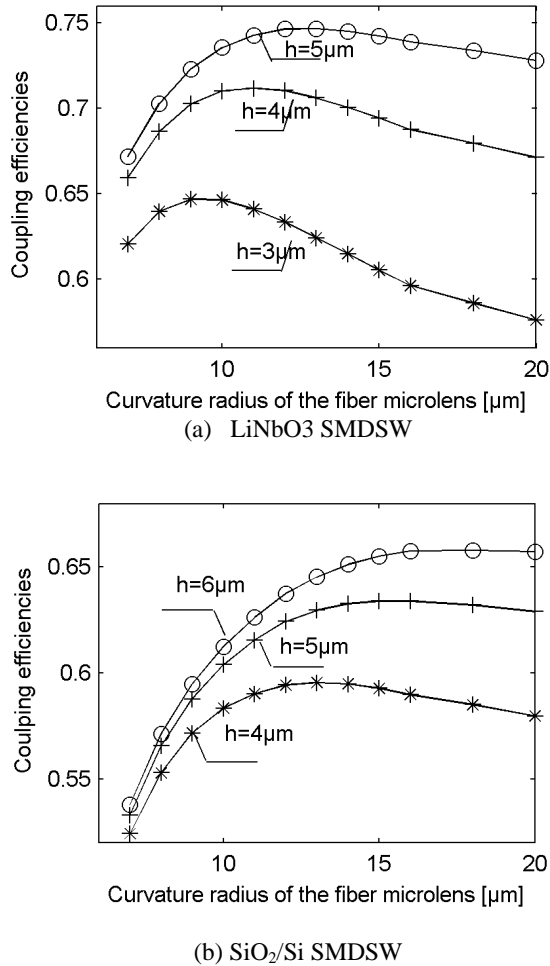


Fig.10. coupling efficiencies for the ended face of the waveguide lying in the waist plane for coupling the SMF to SMDSW with SFML.

To further explain the spherical aberration effect on the coupling efficiency, in the alignment case, the coupling efficiency of a specific SMF coupling to the LiNbO₃ SMDSW with AFFML are shown in Fig.11. When the core thickness of the SMDSW is 5 μ m and the end-face is in the waist plane, the coupling efficiencies are in the region of 65%~81%. The maximum coupling efficiency locates at the point of the focal length of 18 μ m. For butt-joint coupling between the SMF and the SiO₂/Si SMDSW

with a AFFML, the coupling efficiency curves are also shown in Fig.11. The maximum coupling is at the point of the focal length of 25 μ m, and the coupling efficiencies are in the region of 52%-81%.

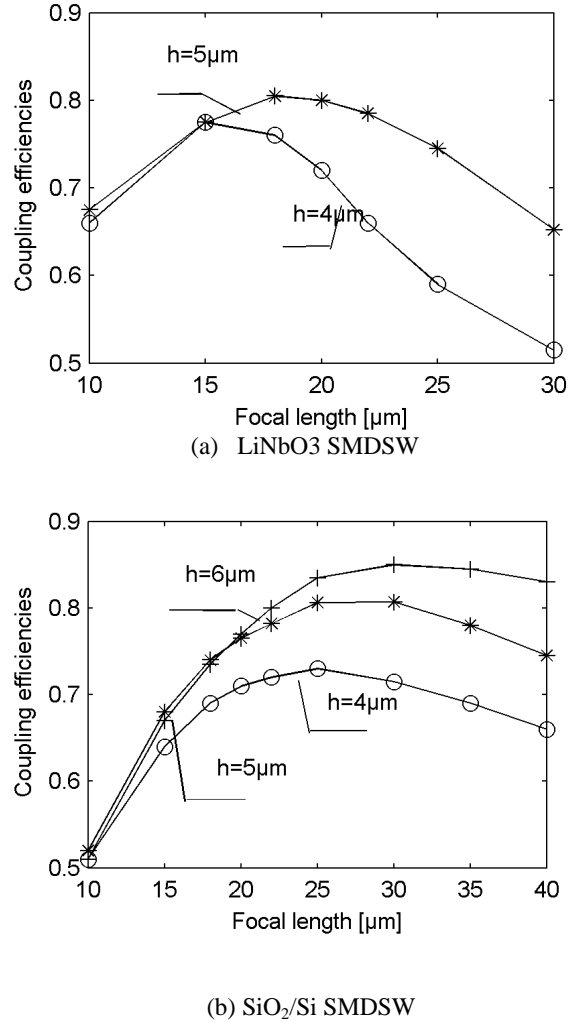


Fig.11. Coupling efficiency for butt-joint coupling between SMF and SMDSW with an AFFML.

From above discussion, for butt joint coupling between the SMF and SMDSW with AFFML, the focal length, which is at the maximum coupling efficiency, is lower than that for butt joint coupling with SFML. The spherical aberration makes the coupling efficiencies less and the curves platter.

7. Conclusions

In this paper, the propagation and coupling characteristics of a SMF and a SMDSW coupling with a SFML is investigated by Monte Carlo simulation method. This method uses the principles of reflection and refraction

at a plane interface between two media, and the diffractions is taken into account too. This treatment can take the primary aberration, fifth order aberration and even the higher order aberration and losses into consideration.

Because of spherical aberration effects, the position of the axial maximum intensity does not coincide with the waist position and the geometrical focus, and the location of the waist is nearer to the geometrical focus for the SFML, and the relative focal shift of the SFML is less than that of the AFFML. And the distribution of the electromagnetic field emerging from the SFML is completely different from that of the SMF. Therefore, the traditional calculating coupling efficiency method, such as overlap integral method, is not valid. For the coupling system of the SMF and the SMDSW coupling with a SFML, the coupling efficiencies less and the curves platter with respect to the AFFML. These simulation results should be helpful for high effective coupling system designing in optical communication.

References

- [1] M. Galarza, K. De Mesel, D. Fuentes, et al, Applied Physics B:Lasers and Optics **73**(5-6), 585 (2001).
- [2] F. Schiappelli, R. Kumar, M. Prasciolu, et al., Microelectronic Engineering **73-74**(1), 397 (2004).
- [3] K. Shiraiishi, M. Kaqaya, K. Muro, H. Yoda, Y. Koqami, S. Tasai Chen, Applied Optics **47**(34), 6345 (2008).
- [4] P. Sun, R. M. Reano, Optics Express **17**(6), 4565 (2009).
- [5] M. Lehtonen, G. Genty, H. Ludvigsen, Applied Physics B: Lasers and Optics **81**(2-3), 295 (2005).
- [6] J. K. Doyle, A. P. Knights, IEEE Journal of Selected Topics in Quantum Electronics **12**(6), 1363 (2006).
- [7] L. Yang, D. X. Dai, B. Yang, Z. Sheng, S. L. He, Applied Optics **48**(4), 672 (2009).
- [8] S. Ríos, R. Srivastava, C. Gómez-Reino, Optics Communications **119**(5-6), 517 (1995).
- [9] A. Yariv, optical electronics in modern communications (Fifth edition), publishing House of Electronics Industry, Beijing,2002,p97
- [10] Y. J., Journal of Modern Optics **39**(8), 1761 (1992).

*Corresponding author: jpzhu@mail.xjtu.edu.cn